Large Signal Model of TDM-Pumped Raman Fiber Amplifier

Miroslav Karásek, Jiři Kaňka, Jan Radil, and Josef Vojtěch

***Abstract*—In this letter, we study spectral optical signal-to-noise ratio (OSNR) profile of a wide-band Raman fiber amplifier (RFA)with time-division-multiplexed (TDM) pumping. We derive a comprehensive large-signal numerical model which incorporates time variation effects and the downstream propagation of signals, upstream propagation of pumps, and downstream and upstream propagation of amplified spontaneous emission spectral components. We present results for a four-wavelength-pumped discrete RFA with TDM and continuous-wave pumping. Improvement in OSNR flatness of 0.9 dB due to TDM pumping is demonstrated.**

***Index Terms*—Optical fiber amplifiers, Raman amplification, time-division multiplexing (TDM).**

I. Introduction

Wavelength-division-multiplexed (WDM) pumping has been proposed to achieve flat Raman gain over an amplification band approaching 100 nm, [1], [2]. In these conventional multiwavelength-pumped Raman fiber amplifiers (RFAs), pump lasers operate continuously at predetermined and optimized wavelengths and powers to generate flat gain-spectral characteristic. Due to pump-to-pump Raman interactions, the longer wavelength pumps are amplified by the shorter wavelength ones and penetrate deeper into the transmission fiber. In counter-directionally pumped RFA, the longer wavelength signals, therefore, encounter Raman gain earlier during their propagation through the Raman fiber than the shorter wavelength counterparts. This results in almost linear wavelength variation of optical signal-to-noise ratio (OSNR). Although the gain spectrum is flat, noise of the shorter wavelength signals is deteriorated by stronger amplified spontaneous emission (ASE). Moreover, strong products of four-wave mixing between the pumps can fall in the signal band when dispersion-shifted fiber (DSF) is used for Raman amplification.

To overcome the above mentioned deficiencies of the WDM continuously pumped wide-band RFA, time-division multiplexing (TDM) of pumps has been suggested and verified experimentally [3]–[6]. Two different approaches to TDM pumping scheme are in principle possible: A single but tunable laser was used as a pump source which was periodically and repetitively swept across a required wavelength range with a certain wavelength pattern [3], [4]. To achieve flat gain spectrum, the wavelength pattern and time spent at individual wavelengths must be optimized. In the second approach, several fixed wavelength lasers were optically combined together as in the case of WDM continuous-wave (CW) pumping but individual lasers were operated in pulsed regime at separate times slots [5]. Both the above mentioned TDM techniques guarantee that at a given spot of the Raman fiber and at a particular time instant, pump wave of only one wavelength is present so that pump-to-pump Raman interactions are avoided. Repetition rate requirements for TDM Raman pumping were quantified, both theoretically and experimentally, in [6]. It has been shown that in order to achieve temporal Raman gain variations less than 1 dB at an average ON–OFF Raman gain of 15 dB in 100 km of nonzero DSF, the repetition rate must be higher than 10 kHz. The analytical model of TDM-pumped RFA presented in [6] is based on the assumption that the Raman fiber length is much longer than its inverse pump attenuation coefficient. Moreover, the model does not take into account signal-to-signal interactions and its application is limited to calculate temporal gain variations of one signal pumped by a single pump only.

In this letter, we present a large-signal numerical model of TDM-pumped RFA. Performance of the model is demonstrated by simulation of wide-band four-wavelength-pumped discrete RFA. Optical properties of the TDM-pumped RFA are compared with an equivalent CW-pumped RFA and improved flatness of the OSNR is demonstrated. In contrast to [6], our numerical model enables us to analyze the behavior of a wide-band TDM-pumped RFA, including calculation of spectral dependence of the OSNR.

II. Numerical Model

The TDM-pumped RFA model used for the simulation is derived from the dynamic model of RFA which was described in detail in [7]. The model is based on the solution of a set of coupled partial differential equations describing propagation of pumps, signals, and both the downstream and upstream propagating spectral components of ASE powers in RFA. The set of coupled partial differential equations for forward and backward propagating pumps, signals, and spectral components of ASE powers $P^{+}(z,t,\nu)$, $P^{-}(z,t,\nu)$ describing their evolution in space and time acquire the form [8].

$$\begin{aligned}\frac{\partial P^{\pm}(z,t,\nu)}{\partial z} &\mp \frac{1}{V_g(\nu)}\frac{\partial P^{\pm}(z,t,\nu)}{\partial t}\\ &= \mp\alpha(\nu)P^{\pm}(z,t,\nu) \pm \gamma(\nu)P^{\mp}(z,t,\nu)\\ &\quad \pm P^{\pm}(z,t,\nu)\end{aligned}$$

Manuscript received March 30, 2005; revised April 25, 2005. This work was supported in part by the Grant Agency of the Czech Republic under Project 102/04/0773 and in part by the Academy of Sciences of Czech Republic under Project 1ET300670503.

M. Karásk and J. Kaňka are with the Institute of Radio Engineering and Electronics, Academy of Sciences of the Czech Republic, Prague 182 51, Czech Republic.

J. Radil and J. Vojtěch are with CESNET a.l.e., Prague 160 00, Czech Republic.

Digital Object Identifier 10.1109/LPT.2005.851888

$$
\begin{aligned}
&\cdot \sum_{\xi>\nu} \frac{g_R(\nu-\xi)}{K_{\text{eff}} A_{\text{eff}}(\nu)} \cdot [P^{\pm}(z,t,\xi) + P^{\mp}(z,t,\xi)] \\
&\pm h\nu \sum_{\xi>\nu} \frac{g_R(\nu-\xi)}{A_{\text{eff}}(\nu)} \cdot [P^{\pm}(z,t,\xi) + P^{\mp}(z,t,\xi)] \\
&\cdot \left[1 + \frac{1}{e^{h(\xi-\nu)/kT} - 1}\right] \Delta\nu \mp P^{\pm}(z,t,\nu) \\
&\cdot \sum_{\xi<\nu} \frac{\nu}{\xi} \frac{g_R(\nu-\xi)}{K_{\text{eff}} A_{\text{eff}}(\nu)} \cdot [P^{\pm}(z,t,\xi) + P^{\mp}(z,t,\xi)] \\
&\mp 2h\nu P^{\pm}(z,t,\nu) \cdot \sum_{\xi<\nu} \frac{g_R(\nu-\xi)}{A_{\text{eff}}(\nu)} \\
&\cdot \left[1 + \frac{1}{e^{h(\xi-\nu)/kT} - 1}\right] \Delta\nu. \qquad (1)
\end{aligned}
$$

In our simulations, the TDM-pumped RFA is counter-directionally pumped. Therefore, $P^{\pm}(z,t,\nu)$ represents downstream signals, $P_s^{+}(z,t,\nu_s)$, upstream pumps, $P_p^{-}(z,t,\nu_p)$, and downstream and upstream spectral components of ASE power, $P_{\text{ASE}}^{\pm}(z,t,\xi)$, contained in frequency slot $\Delta\nu$. $V_g(\nu)$ is the frequency dependent group velocity, $\alpha(\nu)$ is the fiber background loss, $\gamma(\nu)$ is the Rayleigh back scattering coefficient, $g_R(\nu-\mu)$ is the Raman gain coefficient between waves with frequency ν and μ, K_{eff} is the factor taking into account the polarization relation between pumps and Stokes signals, A_{eff} is the effective interaction area of the fiber, h is the Planck's constant, k is the Boltzman's constant, and T the absolute temperature of the fiber. We assume that the pump pulses have Gaussian shape with amplitudes $P_{p0}(\nu_i)$. Numerical solution to the time-dependent propagation equations starts with the determination of steady-state distributions of signal and ASE powers along the Raman fiber pumped by negligible CW powers. Once the steady-state distribution of forward and backward propagating optical powers is calculated, time evolution of individual optical powers $P^{\pm}(z,\nu,t)$ along the fiber is obtained by direct integration according to (2) with the time variable counter-directional pump powers in the form of Gaussian pulses

$$P^{\pm}(z,\nu,t+\delta t) = P^{\pm}(z,\nu,t) + \frac{\partial P^{\pm}(z,\nu,t)}{\partial t} \cdot \Delta t. \qquad (2)$$

The simulation must be performed over a sufficient number of pump periods so that a new steady-state distribution of all optical powers corresponding to TDM pumping scheme along the full length of the Raman fiber is established.

III. Simulation Results

We will demonstrate the performance of our numerical model on an RFA consisting of 13 km of dispersion-compensation fiber (DCF) counter-directionally pumped at four wavelengths: 1433, 1447, 1470, and 1490 nm. The pump wavelengths have been selected with the aim to amplify 25 WDM channels starting at 1535 nm with 2-nm spacing and input power of $P_{s0} = -7$ dBm/channel. Pump modulation frequency has been set to $f_m = 200$ kHz, high enough to prevent significant signal gain variations [4]. The wavelength-dependent Rayleigh scattering coefficient $\gamma(\lambda) = 2.35\ 10^{-25}/\lambda^3$

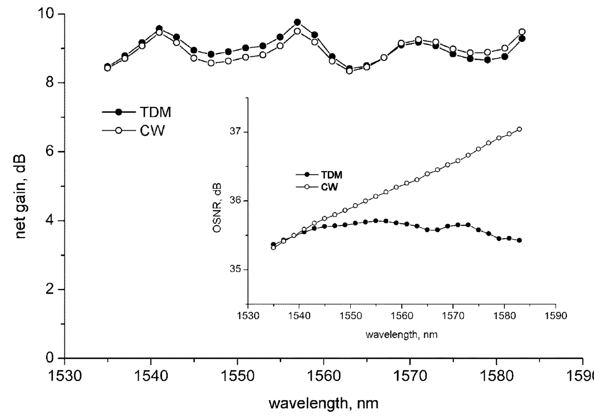

Fig. 1. Spectral dependence of net gain of the CW- and TDM-pumped RFA (inset: spectral dependence of OSNR).

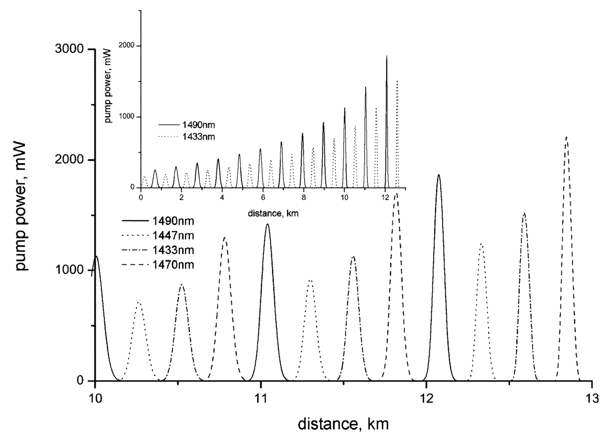

Fig. 2. Distribution of time variable pump power along the DCF fiber: TDM pumping.

[9], empirical quadratic relation for wavelength dependence of DCF loss $\alpha(\lambda) = 1.334 \cdot 10^{-5}\lambda^2 - 0.412\lambda + 32.266$, and the polarization factor between pump and Stokes signals $K_{\text{eff}} = 2$ have been assumed. Using a simple procedure we optimized pulse amplitudes $P_{p0}(\nu_i)$ at individual pump wavelengths under the assumption of equal pulsewidth FWHM $= 0.125\ \mu$s $(i = 1,\ldots,4)$ and total average pump power of $P_{\text{tot}} = 500$ mW. Gain ripple of 10.9% was found for the following pulse amplitudes $P_{p0} = 3.9$, 3.5, 5.6, and 5.6 W at 1433, 1447, 1470, and 1490 nm, respectively. Spectral dependence of net gain is plotted in Fig. 1. Fig. 2 shows the distribution of all four pumps for $10\ \text{km} < z < 13\ \text{km}$ at a certain instant in time. The inset plots the evolution of pump power at 1433 and 1490 nm along the full length of the Raman fiber. Evolution of time averaged pump powers $P_p^{-}(z,\nu_p) = 1/T_m \int_0^{T_m} P_p^{-}(z,\nu_p,t)dt$ along the Raman fiber is plotted in Fig. 3. Fig. 4 shows the time evolution of signal power (1535 nm) at the output of RFA. It is seen that after about 175 μs (35 periods of TDM pumping), a steady state is reached. The inset demonstrates the signal modulation due to TDM pumping. It can be seen that the temporal signal power variation defined as $10\log P_s^{\max}/P_s^{\min}$ is equal to 0.28 dB which is in agreement with the experimental results presented [6, Fig. 7]. In the following, we will compare spectral dependence of net gain and OSNR of the above described TDM-pumped

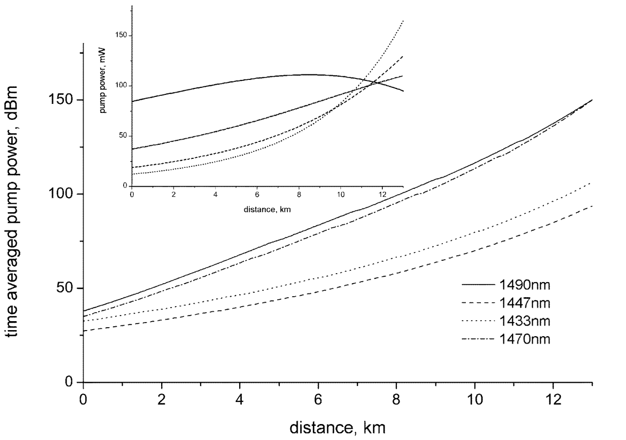

Fig. 3. Distribution of time averaged pump power along the DCF fiber: TDM pumping (inset: distribution of pump power along the DCF fiber: CW pumping).

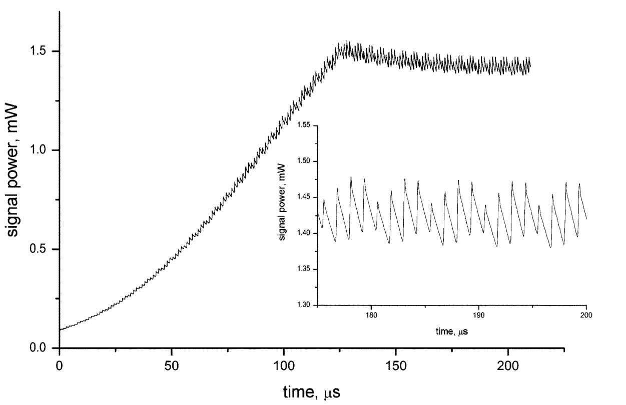

Fig. 4. Time evolution of output signal power at 1535 nm after the TDM pumping is switched ON.

RFA and a CW-pumped RFA deploying the same 13-km-long DCF, the same four pump wavelengths with total power of $P_{\rm tot} = 500$ mW. By trial and error optimization of pump powers, we have found reasonably flat gain spectrum of the above mentioned 25 WDM channels $(\mathrm{GR} = 10.5\%)$ for pump powers of 165, 130, 110, and 95 mW at 1433-, 1447-, 1470-, and 1490-nm pump wavelengths, respectively. The spectral dependence of net gain is shown in Fig. 1. Distribution of pump power along the Raman fiber is shown in the inset of Fig. 3. It is seen that at CW pumping, the longest wavelength pump (1490 nm) is amplified by the shorter wavelength ones and penetrates deep into the signal end of the Raman fiber. The longer wavelength signals encounter the distributed amplification earlier than the shorter wavelength counterparts and exhibit, therefore, higher OSNR. This is demonstrated in the inset of Fig. 1, where the spectral dependence of OSNR is plotted for the TDM- and CW-pumped RFA. The ASE power was calculated with 0.5-nm resolution. The OSNR of the CW-pumped RFA increases with increasing signal wavelength,

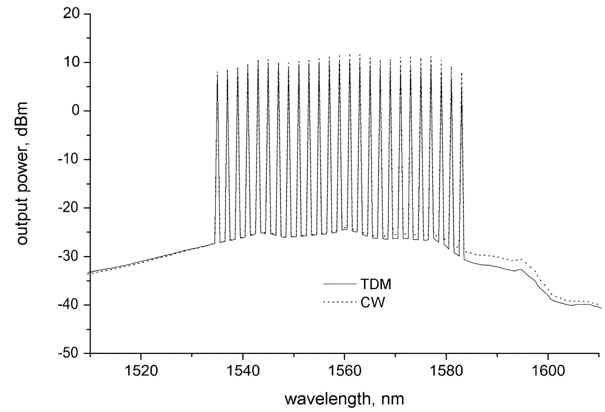

Fig. 5. Spectral dependence of output power.

the difference between the 1535- and 1583-nm channels is 1.7 dB while the OSNR variation of the TDM-pumped RFA is less than 0.4 dB. Spectral dependence of output power for both the TDM and CW-pumped RFA is shown in Fig. 5.

IV. Conclusion

We have demonstrated the performance of a large-signal numerical model for simulation of TDM-pumped RFAs which confirms the advantages of TDM pumping. The model enables us to analyze the effect of pump modulation frequency and duty cycle on the temporal variation of Raman gain. It can be used for the design of wide-band RFA with flattened spectral dependence of OSNR.

References

[1] Y. Emori, K. Tanaka, and S. Nmiki, "100 nm bandwidth flat-gain Raman amplifiers pumped and gain-equalized by 12-wavelength-channel WDM laser diode unit," *Electron. Lett.*, vol. 35, pp. 1355–1356, 1999.

[2] Y. Emori, S. Matsushita, and S. Naminki, "1 THz-spaced multi-wavelength pumping for broad-band Raman amplifiers," in *Proc. ECOC*, vol. 2, 2000, Paper 4.4.2, pp. 73–74.

[3] L. F. Mollenauer, A. R. Grant, and P. V. Mamyshev, "Time-division multiplexing of pump wavelengths to achieve ultrabroadband, flat, backward-pumped Raman gain," *Opt. Lett.*, vol. 27, pp. 592–594, 2002.

[4] P. J. Winzer, K. Sherman, and M. Zirnbibl, "Time-division multiplexed Raman pump experiment using a tunable C-band laser," *IEEE Photon. Technol. Lett.*, vol. 16, no. 6, pp. 789–791, Jun. 2002.

[5] C. R. S. Fludger, V. Handerek, N. Jolley, and R. J. Mears, "Novel ultrabroadband high performance distributed Raman amplifier employing pump modulation," in *Proc. OFC 2002*, 2002, Paper WB4, pp. 183–184.

[6] P. J. Winzer, J. Bromage, R. T. Kane, P. A. Sammer, and C. Headley, "Repetition rate requirements for time-division multiplexed Raman pumping," *J. Lightw. Technol.*, vol. 22, no. 2, pp. 401–408, Feb. 2004.

[7] M. Karasek, J. Kanka, P. Honzatko, and P. Peterka, "Time-domain simulation of power transients in Raman fiber amplifiers," *Int. J. Numerical Modeling*, vol. 17, pp. 165–167, 2004.

[8] S. Namiky and Y. Emori, "Ultrabroad-band Raman amplifiers pumped and gain-equalized by wavelength-division-multiplexed high-powetr laser diodes," *IEEE J. Sel. Topics Quantum Electron.*, vol. 7, no. 1, pp. 3–16, Jan./Feb. 2001.

[9] H. Kidorf, K. Rottwitt, M. Nissov, M. Ma, and E. Rabarijaona, "Pump interactions in a 100-nm bandwidth Raman amplifier," *IEEE Photon. Technol. Lett.*, vol. 11, no. 5, pp. 530–532, May 1999.